Epitaxial Overgrowth of Gallium Nitride Nano-Rods on Silicon (111) Substrates by RF-Plasma-Assisted Molecular Beam Epitaxy



2010 Jpn. J. Appl. Phys. 49 04DH06

(http://iopscience.iop.org/1347-4065/49/4S/04DH06)

# Epitaxial Overgrowth of Gallium Nitride Nano-Rods on Silicon (111) Substrates by RF-Plasma-Assisted Molecular Beam Epitaxy

Jui-Tai Ku, Tsung-Hsi Yang[1,2], Jet-Rung Chang[1], Yuen-Yee Wong[3], Wu-Ching Chou*, Chun-Yen Chang[1,2], and Chiang-Yao Chen[4]

*Department of Electrophysics, National Chiao Tung University, Hsinchu, Taiwan 30010, R.O.C.*
[1]*Department of Electronics Engineering, National Chiao Tung University, Hsinchu, Taiwan 30010, R.O.C.*
[2]*Microelectronics and Information Systems Research Center, National Chiao Tung University, Hsinchu, Taiwan 30010, R.O.C.*
[3]*Department of Materials Science and Engineering, National Chiao Tung University, Hsinchu, Taiwan 30010, R.O.C.*
[4]*Ulvac Taiwan Inc., Hsinchu, Taiwan 30078, R.O.C.*

Received October 5, 2009; accepted November 26, 2009; published online April 20, 2010

Strain-free gallium nitride (GaN) overgrowth on GaN nano-rods is realized by RF-plasma assisted molecular beam epitaxy (RF-MBE) on silicon (Si) substrate. The strain-free condition was identified by the strong free A exciton ($FX_A$) photoluminescence (PL) peak at 3.478 eV and the $E_2$ high phonon Raman shift of 567 $cm^{-1}$. It is clearly demonstrated that the critical diameter of GaN nano-rods is around 80 nm for the overgrowth of strain-free GaN. The blue-shift of PL peak energy and phonon Raman energy with decreasing the diameter of nano-rod result from the strain relaxation of overgrowth GaN. 

DOI: 10.1143/JJAP.49.04DH06

## 1. Introduction

Group-III–nitride semiconductors such as aluminum nitride (AlN), gallium nitride (GaN), indium nitride (InN) and their ternary alloys has applications in high-electron mobility transistor devices (HEMTs)[1)] and light emitting devices (LEDs) operating in the UV–visible range.[2)] Most devices are prepared by metal organic chemical vapor deposition (MOCVD) using sapphire or SiC as substrates. Recently, GaN grown on Si substrate has attracted considerable academic and commercial attention because of its lower cost, larger sizes, higher crystalline quality and great potential for mature device processing and device integration with Si circuitry. However, growing device-quality GaN epilayers on Si substrates are challenging because of the large differences in the lattice constant (20%) and thermal expansion coefficient (56%) between GaN and Si, which lead to high dislocation density ($10^8$–$10^{10}$ $cm^{-2}$) and strain induced piezo-polarization field and further degrade the electrical and optical properties of the devices. Furthermore when thickness of nitride layers exceeds 1.0 μm, a lot of cracks were observed in the film. A number of approaches to grow GaN layers with reduced density of crack and threading dislocation (TD) have been reported. The overgrowth GaN on the patterned $SiO_2$ mask drastically reduced the TD density.[3,4)] The structural characteristics of the GaN epitaxial films grown on the patterned sapphire[5)] and Si substrate[6)] were also found to be improved effectively. Recently, the TD of GaN overgrowth layer on the patterned GaN nano-column[7–9)] can be further reduced down to $10^7$ $cm^{-2}$. However, the high-cost and time-consuming etching process to produce the patterned substrates or nano-column is the major drawback. To overcome the problem, GaN epitaxial films could be overgrown on the GaN nano-rods which are self-organized on Si substrate at a reduced Ga surface diffusion under nitrogen rich condition.[10)] The GaN nano-rods have nice crystal quality and are perpendicular to the Si substrates.[11)] The GaN nano-rods of typically 20–200 nm in diameter and 0.2–2.0 μm in height with a density of $(0.2–1.8) \times 10^{10}$ $cm^{-2}$ could be grown by modulation the growth parameters such as III/V ratio, substrate's temperature and thickness of buffer layer.[12,13)] Kusakabe *et al.*[14)] grew the freestanding GaN film of high crystal quality and nearly no residual strain on (0001) sapphire substrates using self-organized GaN nano-rods buffer by RF-plasma assisted molecular beam epitaxy (RF-MBE). Chern *et al.*[15)] show that the nano-rods remain free of TDs until coalescence.

In this work, GaN nano-rods of different diameters were grown by RF-MBE as buffer layers. GaN films were grown on top of the GaN nano-rods to reduce TD and relax the strain. The diameters of the GaN nano-rods were controlled by adjusting the III/V flux ratio to searching for best condition for GaN epitaxial overgrowth. The strain free GaN layer overgrowth on self-organized GaN nano-rods/Si(111) substrates by RF-MBE was verified by low temperature photoluminescence (PL) and Raman scattering analysis. It is clearly demonstrated that the critical diameter of GaN nano-rods for overgrowth strain-free GaN was determined as around 80 nm.

## 2. Experimental Procedure

The GaN nano-rods of different diameters and the overgrowth GaN layers were grown sequentially on the Si(111) substrates by ULVAC RF-MBE system with liquid nitrogen cryo-panel cooling. The 2-in. Si(111) wafers (p-type doping) were chemically cleaned by 10% HF without rinsing in deionized (DI) water to suppress oxide formation. A clear Si(7×7) surface reconstruction was observed by the reflection high-energy electron diffraction (RHEED) at a substrate temperature of 830 °C. The GaN nano-rods were then directly grown on Si(111) substrates at 850 °C without any buffer layer under different III/V ratios to control the diameters of GaN nano-rods. During the growth, the RF-plasma power and nitrogen flow rate were kept constant at 500 W and 4.0 sccm, respectively. The variation of III/V flux ratio was adjusted by the Ga flux. The Ga flux was varied from $9.0 \times 10^{-8}$, $1.9 \times 10^{-7}$ to $3.7 \times 10^{-7}$ Torr for samples A, B, and C, respectively. The respective rod diameters of 60, 80, and 90 nm were investigated by JEOL JSM-7001F scanning electron microscopy (SEM). Followed the growth of GaN nano-rods, the Ga flux was increased to

*E-mail address: wuchingchou@mail.nctu.edu.tw

 

$9.7 \times 10^{-7}$ Torr to enhance the lateral growth rate for the growth of the overgrowth GaN layers. The detailed growth process was described elsewhere.[16] The optical property was examined by PL measurement. The 325 nm He–Cd laser was used as an excitation light source. The PL signal was analyzed by a 0.85 m SPEX-1403 double-grating spectrometer equipped with a photomultiplier tube. The residual strain in overgrowth GaN layers was evaluated by micro-Raman scattering at room temperature in backscattering geometry along the $z$-direction (parallel to the $c$-axis of GaN). The 488 nm line of an $Ar^+$-ion laser was used as the excitation source and focused through a microscope (Olympus BX41) objective into a spot of around 1 μm in diameter. The spectra were obtained using a 0.85 m SPEX-1404 double-grating (1800 grooves/mm grating) spectrometer equipped with a multichannel $LN_2$-cooled charge-coupled device (CCD) of $1024 \times 256$ pixels. The pixel size of $26 \times 26\,\mu m^2$ yields spectral resolution better than $1.25\,cm^{-1}$. The lattice constant of GaN was determined by high-resolution X-ray diffraction (HRXRD) on a Bede D1 system using the Cu $K\alpha_1$ line.

## 3. Results and Discussion

Figures 1 and 2 show the cross-sectional and top-view SEM images of overgrowth GaN with different nano-rod diameters. The diameters of samples A, B, and C are (a) 60, (b) 80, and (c) 90 nm, respectively. The N-rich nano-rod layers and the Ga-rich overgrowth layers can be clearly identified from the cross-section SEM images of Fig. 1. As the Ga flux was increased, the lateral overgrowth was enhanced. For sample A, the overgrowth GaN forms irregular terraces and without fully coalescence as shown in Fig. 2(a). By increasing the diameters of nano-rods, the gaps between the nano-rods decrease. The GaN terraces merge together to show better surface morphology in Figs. 2(b) and 2(c). The cross-sectional SEM image of sample B shows that the film is not continuous in lateral direction, and from boundaries gaps. From the top-view SEM image, one can see the spacing gradually shrunk as the diameter of nano-rods was increased and the area of the terrace was also increased, as show in Fig. 2(b). The further increasing diameter of nano-rods results in continuous morphology in cross-section of sample C as shown in Fig. 1(c). In Fig. 2(c), the top-view SEM image shows that the overgrowth layer in sample C is not completely continuous, with pronounced trenches and some pits.

Figure 3 show the low-temperature (10 K) normalized PL spectra of three samples. Because the much lower PL probing depth at 325 nm excitation,[17,18] the signals is primarily from the overgrowth layer. All three spectra are dominated by the strong narrow near-band-edge (NBE) excitonic emission near 3.47 eV and a weak broad emission from 3.32 to 3.42 eV. No deep-level emission or yellow-band transition at 2.3 eV was detected. The two main peaks of the weak emission band are assigned to the excitons bound to surface defect ($Y_2$) and the shallow donor–acceptor pair (DAP) located on surface ($Y_6$).[19] The broad emission is relatively weak in sample C, which has smooth surface morphology. It implies the smooth surface reduces the surface defects.

In order to further identify the emission mechanism, the temperature-dependent PL experiments at temperature range from 10 to 120 K are presented in Fig. 4. In Fig. 4, the weak shoulder at 3.485 eV is attributed to the free B exciton transition ($FX_B$). The strongest peak at 3.478 eV is identified as the free A exciton transition ($FX_A$). The peak at 3.472 eV results from the recombination of A exciton bound to neutral donor ($D^0X_A$). The energy red-shift with temperature of $FX_A$ follows the Vashini's equation. For $D^0X_A$ peak, the intensity decrease abruptly due to the thermal excitation to higher energy $FX_A$ state. The thermal quenching of the donor-bound exciton ($D^0X_A$) peak occurs at 80–100 K.[20] For sample A and B, the energy position of $FX_A$ at 3.478 eV implies that the overgrowth GaN is strain-free.[21] The $FX_A$ stronger than $D^0X_A$ also show that the overgrowth GaN is high quality with low density of defects, which was only observed in high-quality single-crystal nano-rod.[22] On the other hand, the PL spectrum of sample C was dominated by the $D^0X_A$ transition at 3.466 eV, shown in Fig. 4(c). Compare with the energy position of $D^0X_A$ of samples A and B, the energy of $D^0X_A$ for sample C red-shifts 6 meV. This indicates that the overgrowth GaN of sample C has tensile strain. By using the value of the proportionality factor

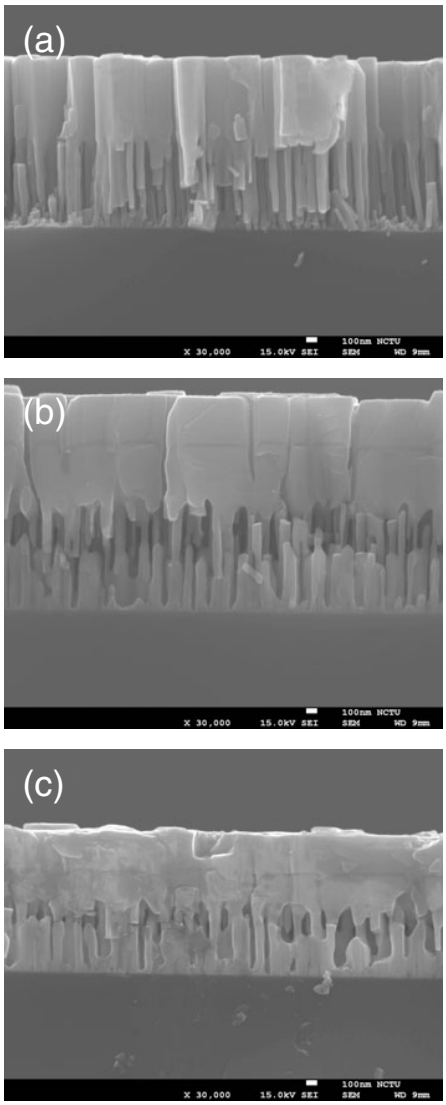


**Fig. 1.** Cross-sectional SEM images of the overgrowth sample. The diameters for samples A to C are (a) 60, (b) 80, and (c) 90 nm, respectively. The scale bars are 100 nm.

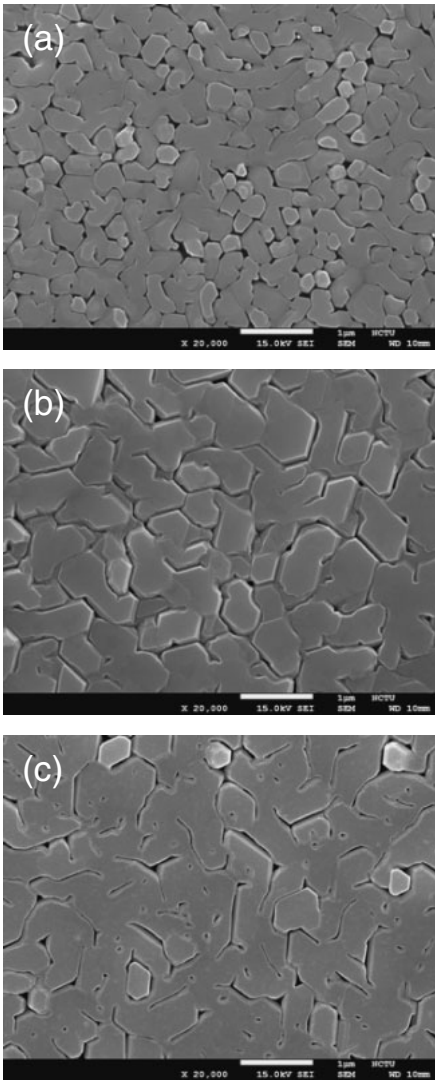


**Fig. 2.** Top-view SEM images of the overgrowth GaN: (a) sample A, (b) sample B, and (c) sample C. The scale bars are 1 μm.

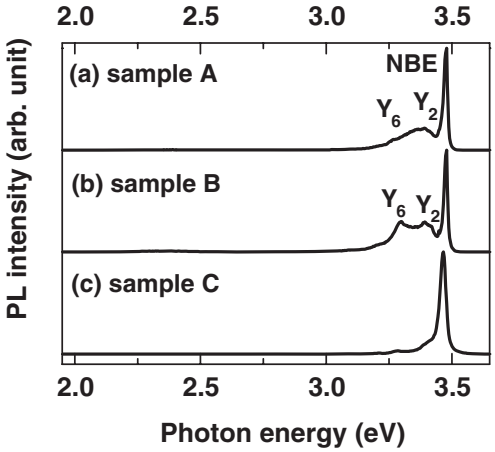


**Fig. 3.** Low-temperature (10 K) normalized PL spectra.

$K = 21.2\,\mathrm{meV/GPa}$[23] for the strain-induced PL peak shift, a residual stress of 0.28 GPa built in the overgrowth layer can be estimated.

The tensile strain in these specimens was also investigated by the micro-Raman spectroscopy by measuring the frequency position of the $E_2$-high phonon mode. The normalized $E_2$-high mode of these specimens measured at room temperature is shown in Fig. 5. The peak of Raman shift in samples A, B, and C are 567.0, 567.0, and 565.7 $\mathrm{cm^{-1}}$, respectively. The energy positions of $E_2$-high peak for samples A and B are at $567.0 \pm 0.1\,\mathrm{cm^{-1}}$, which is believed to be the $E_2$-phonon from strain-free GaN.[24] The energy difference in the Raman shift between sample C and sample A (and sample B) is $1.3\,\mathrm{cm^{-1}}$. The residual stress could be calculated based on the stress coefficient of $4.24\,\mathrm{cm^{-1}\,GPa^{-1}}$.[24] The estimated residual stress in the overgrowth GaN layer of sample C is 0.30 GPa, which is quite consistent with the result of PL spectral shift. The redshift of PL peak energy and Raman shift value in sample C is due to the residual biaxial compressive stress in the *c*-plane of GaN and induced tensile uniaxial strain along the *c*-axis.

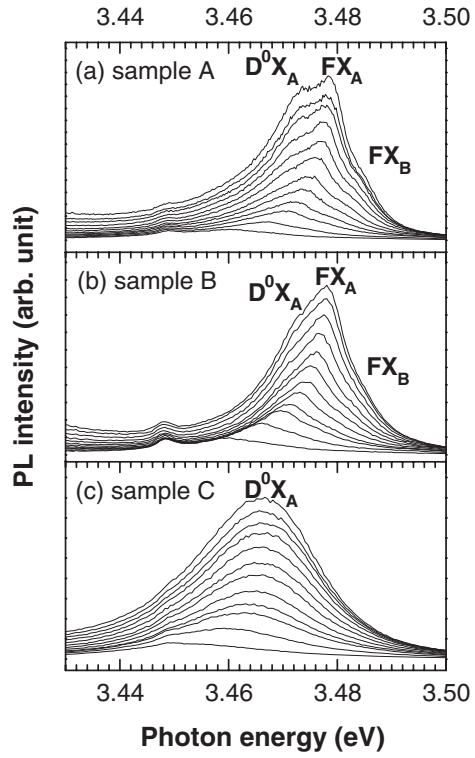


**Fig. 4.** Temperature-dependent PL spectra of three samples.

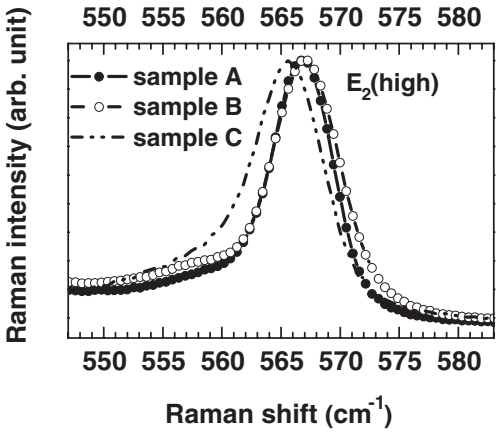


**Fig. 5.** Room-temperature normalized Raman scattering spectra of three samples.

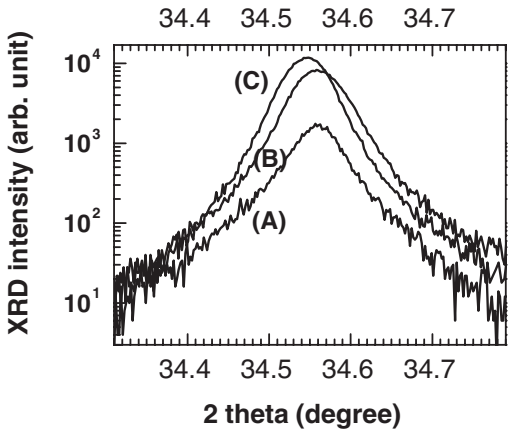


**Fig. 6.** X-ray 2$\theta$-scans of the symmetric (0002) diffraction for samples A–C.

This residual stress can be further checked by measuring the X-ray 2$\theta$-scan of (0002) diffraction. The respective peak positions of XRD for samples A, B, and C are at 34.560, 34.560, and 34.546°, as shown in Fig. 6. The calculated $c$-axis lattice constants of samples A, B, and C are 5.1844, 5.1844, and 5.1864 Å, respectively. The $c$-axis lattice constants of samples A and B are very close to the strain-free value of $c_0 = 5.185$ Å. The larger $c$-axis lattice constant of sample C indicates the existence of tensile strain along the $c$-axis of GaN. The in-plane stress ($\sigma$) of GaN grown on Si can be described by the lattice strain ($\varepsilon$) from the relationship $\sigma = M\varepsilon$, where $M$ is the biaxial elastic modulus of GaN. When the hexagonal GaN is bi-axially stressed on Si, its in-plane lattice deformation ($\varepsilon_a$) is associated with out-of-plane lattice change ($\varepsilon_c$) by the relationship $\varepsilon_c = -2(C_{13}/C_{33})\varepsilon_a$, where $\varepsilon_c = (c - c_0)/c_0$ and $C_{13}$, $C_{33}$ are the elastic constants of GaN.[25] The in-plane biaxial stress in sample C can be calculated by using $M = 449$ GPa, $C_{13} = 103$ GPa, and $C_{33} = 405$ GPa,[26] respectively. The estimated biaxial compressive stress in the $c$-plane of sample C is 0.24 GPa, which is quite consistent with the results of PL and Raman measurements.

From the results of Figs. 4–6, one can conclude that residual strain will exist in the GaN overgrowth on GaN nano-rods of diameter larger than 90 nm. We propose that the initially nucleation behavior of large size GaN nano-rods is consistent with the strained GaN quantum dots (QDs).[27] This is due to the relatively higher Ga/N ratio of large size GaN nano-rods. This indicates that only suitable diameter of GaN nano-rod can be used as a buffer layer for overgrowth strain-free GaN layer.

## 4. Conclusions

In conclusion, we have demonstrated the growth of high quality coalescence overgrowth GaN nano-rods on Si(111) substrate with RF-MBE. By using the temperature-dependent PL experiments and micro-Raman spectroscopy, the critical diameter of GaN nano-rods for strain-free GaN overgrowth is around 80–90 nm. The residual stress which exists in GaN overgrown on GaN nano-rods with 90 nm of diameter is about 0.3 GPa.

## Acknowledgements

This work was supported by the National Science Council of Taiwan under the grant number of NSC 96-2221-E-009-202-MY3, NSC 97-2221-E-009-153, NSC 98-2221-E-009-003, and NSC 96-2112-M-009-026-MY3. We also would like to thank ULVAC Taiwan for maintenance supporting.

1) E. Bahat-Treidel, R. Lossy, J. Würfl, and G. Tränkle: IEEE Electron Device Lett. **30** (2009) 901.
2) M. Funato, T. Kondou, K. Hayashi, S. Nishiura, M. Ueda, Y. Kawakami, Y. Narukawa, and T. Mukai: Appl. Phys. Express **1** (2008) 011106.
3) O. H. Nam, M. D. Bremser, T. S. Zheleva, and R. F. Davis: Appl. Phys. Lett. **71** (1997) 2638.
4) K. Y. Zang, Y. D. Wang, S. J. Chua, and L. S. Wang: Appl. Phys. Lett. **87** (2005) 193106.
5) J. Wang, L. W. Guo, H. Q. Jia, Y. Wang, Z. G. Xing, W. Li, H. Chen, and J. M. Zhou: J. Electrochem. Soc. **153** (2006) C182.
6) K. Y. Zang, Y. D. Wang, S. J. Chua, L. S. Wang, S. Tripathy, and C. V. Thompson: Appl. Phys. Lett. **88** (2006) 141925.
7) Y. D. Wang, K. Y. Zang, S. J. Chua, S. Tripathy, H. L. Zhou, and C. G. Fonstad: Appl. Phys. Lett. **88** (2006) 211908.
8) C. L. Chao, C. H. Chiu, Y. J. Lee, H. C. Kuo, P. C. Liu, J. D. Tsay, and S. J. Cheng: Appl. Phys. Lett. **95** (2009) 051905.
9) Y. S. Chen, W. Y. Shiao, T. Y. Tang, W. M. Chang, C. H. Liao, C. H. Lin, K. C. Shen, C. C. Yang, M. C. Hsu, J. H. Yeh, and T. C. Hsu: J. Appl. Phys. **106** (2009) 023521.
10) M. Yoshizawa, A. Kikuchi, M. Mori, N. Fujita, and K. Kishino: Jpn. J. Appl. Phys. **36** (1997) L459.
11) J. E. Van Nostranda, K. L. Averett, R. Cortez, J. Boeckl, C. E. Stutz, N. A. Sanford, A. V. Davydov, and J. D. Albrecht: J. Cryst. Growth **287** (2006) 500.
12) C. L. Hsiao, L. W. Tu, T. W. Chi, H. W. Seo, Q. Y. Chen, and W. K. Chu: J. Vac. Sci. Technol. B **24** (2006) 845.
13) R. Calarco, R. J. Meijers, R. K. Debnath, T. Stoica, E. Sutter, and H. Lth: Nano Lett. **7** (2007) 2248.
14) K. Kuskabe, A. Kikuchi, and K. Kishino: Jpn. J. Appl. Phys. **40** (2001) L192.
15) D. Cherns, L. Meshi, I. Griffiths, S. Khongphetsak, S. V. Novikov, N. Farley, R. P. Campion, and C. T. Foxon: Appl. Phys. Lett. **92** (2008) 121902.
16) T. H. Yang, J. T. Ku, J. R. Chang, S. G. Shen, Y. C. Chen, Y. Y. Wong, W. C. Chou, C. Y. Chen, and C. Y. Chang: J. Cryst. Growth **311** (2009) 1997.
17) J. F. Muth, J. H. Lee, I. K. Shmagin, R. M. Kolbas, H. C. Casey, Jr., B. P. Keller, U. K. Mishra, and S. P. DenBaars: Appl. Phys. Lett. **71** (1997) 2572.
18) A. Kar, D. Alexson, M. Dutta, and M. A. Stroscio: J. Appl. Phys. **104** (2008) 073502.
19) M. A. Reshchikov and H. Morkoç: J. Appl. Phys. **97** (2005) 061301.
20) V. Kirilyuk, P. R. Hageman, P. C. M. Christianen, P. K. Larsen, and M. Zielinski: Appl. Phys. Lett. **79** (2001) 4109.
21) P. P. Paskov, T. Paskova, P. O. Holtz, and B. Monemar: Phys. Rev. B **70** (2004) 035210.
22) M. Tchernycheva, C. Sartel, G. Cirlin, L. Travers, G. Patriarche, J. C. Harmand, L. S. Dang, J. Renard, B. Gayral, L. Nevou, and F. Julien: Nanotechnology **18** (2007) 385306.
23) D. G. Zhao, S. J. Xu, M. H. Xie, S. Y. Tong, and Hui Yang: Appl. Phys. Lett. **83** (2003) 677.
24) A. R. Goñi, H. Siegle, K. Syassen, C. Thomsen, and J.-M. Wagner: Phys. Rev. B **64** (2001) 035205.
25) A. Krost, A. Dadgar, G. Strassburger, and R. Clos: Phys. Status Solidi A **200** (2003) 26.
26) A. F. Wright: J. Appl. Phys. **82** (1997) 2833.
27) O. Landré, C. Bougerol, H. Renevier, and B. Daudin: Nanotechnology **20** (2009) 415602.